# AIP Advances

# The effect of ice type on ice adhesion

Sigrid Rønneberg, Caroline Laforte (ID), Christophe Volat, Jianying He (ID), and Zhiliang Zhang (ID)

View Online        Export Citation        CrossMark

## ARTICLES YOU MAY BE INTERESTED IN

Superhydrophobic surfaces cannot reduce ice adhesion
Applied Physics Letters **101**, 111603 (2012); https://doi.org/10.1063/1.4752436

Frost formation and ice adhesion on superhydrophobic surfaces
Applied Physics Letters **97**, 234102 (2010); https://doi.org/10.1063/1.3524513

Strain engineering in functional materials
AIP Advances **9**, 030701 (2019); https://doi.org/10.1063/1.5075637

# The effect of ice type on ice adhesion

View Online    Export Citation    CrossMark

Sigrid Rønneberg,[1] Caroline Laforte,[2] (iD) Christophe Volat,[2] Jianying He,[1] (iD) and Zhiliang Zhang[1,a] (iD)

## AFFILIATIONS

[1] Department of Structural Engineering, Norwegian University for Science and Technology (NTNU), NO-7491 Trondheim, Norway
[2] Anti-Icing Materials International Laboratory (AMIL), Université du Québec à Chicoutimi, 555 Blvd. de l'Université, Chicoutimi, Québec G7H 2B1, Canada

[a] Corresponding author. E-mail: zhiliang.zhang@ntnu.no. **Telephone:** +4773592530 / +4793001979

## ABSTRACT

To lower the ice adhesion strength is the most efficient technique for passive ice removal for several applications. In this paper, the effect of different types of ice on the ice adhesion strength was investigated. The ice types precipitation ice, in-cloud ice and bulk water ice on the same aluminum substrate and under similar environmental conditions were investigated. The ice adhesion strength was measured with a centrifugal adhesion test and varied from $0.78 \pm 0.10$ MPa for precipitation ice, $0.53 \pm 0.12$ MPa for in-cloud ice to $0.28 \pm 0.08$ MPa for bulk water ice. The results indicate that the ice adhesion strength inversely correlates with the density of ice. The results inspire a new strategy in icephobic surface development, specifically tailored to the relevant ice type.

## I. INTRODUCTION

Ice removal is necessary to avoid both dangerous situations[1–5] and the unwanted icing of infrastructure[6–10] and aircrafts.[11,12] The most promising strategy for creating anti-icing surfaces[1,9,13–15] are the lowering of ice adhesion strength.[16–18] With a low ice adhesion strength, the ice formed on a surface might be shed off merely due to natural vibrations, its own weight or naturally occurring wind.[18,19] Such a reduction requires a thorough understanding of the mechanisms of ice-solid adhesion. However, the fundamental physics of ice adhesion are not yet well understood.[4]

When measuring ice adhesion strength, there are several available methods.[10,20–22] As of today, there is no testing standard, and each research group often develops its own testing techniques.[20,23,24] Ice adhesion strength data measured at different laboratories can therefore not be easily compared.[20,25,26] The choice of an efficient testing method depends on both the ice sample, and the type of surface to be tested. Different surfaces have different adhesion mechanisms to ice, which closely link with the ice removal process.[27] The size, chemical and mechanical properties, and the realistic icing conditions prevailing in the targeted application of the anti-icing surface are also important to determine the most efficient testing method.

The adhesion strength of ice Ih, which is the relevant ice phase for anti-icing applications, depends on many factors. These factors include the surface chemistry, the surface roughness profile, the elastic modulus, the temperature, and the ice micro-structure.[5,27] The type of accreted ice is an important factor in the measurement of ice adhesion strength.[25] When water freezes in various atmospheric conditions, different types of ice are generated.[4,5,10,14,20] These different types of ice vary in micro-structures and densities,[28] and behave in different manners when adhering to any given surface.[22,25] Among the applications of anti-icing, there is a need to remove several different types of ice depending on icing conditions. For example, the ice that is accreted on aircrafts during flight, on roads, and on power transmission lines are different, with different accretion mechanisms. As a result, it is a limitation of most laboratory work that only one type of ice is tested for anti-icing surfaces in each laboratory with the same measurement techniques.

The present investigation aims to understand the difference in adhesion strength between different types of ice. Precipitation ice from a simulation of atmospheric precipitation, impact ice from in-cloud icing and bulk water ice were generated on the same substrate at the same air temperature and removed by the same ice adhesion strength test method. The results indicate that the ice type has

TABLE I. Definition of ice types and ice generation methods.

| Ice # | Name | Type of ice | Generation method |
|---|---|---|---|
| Ice 1 | Precipitation ice | Hard rime ice | Super-cooled precipitation in a cold room |
| Ice 2 | In-cloud ice | Impact ice | Super-cooled micro-droplets in a wind tunnel |
| Ice 3 | Bulk water ice | Clear ice | Frozen water in silicon molds in a cold room |

a clear effect on adhesion strength. This difference of ice adhesion strength is attributed to the density. The findings from this study inspire a new strategy in icephobic surface design and development. For instance, a future surface might be tailored to repel a certain type of ice, depending on the application.

## II. EXPERIMENTAL METHODS

The experimental work was performed at the Anti-icing Materials International Laboratory (AMIL) in Chicoutimi, Canada, which is the only laboratory in the world approved by ISO 9001:2015, PRI AC3001 and PRI AC3002 to qualify de-icing and anti-icing products for aircraft applications.[29] The experiments conducted here consist of more than 120 measurements of ice adhesion strength with a centrifugal adhesion test (CAT) and three types of ice at the same temperature. The generation of ice will be detailed first, before the CAT procedure is explained.

### A. Generation of ice samples

The three types of ice generated in this study were precipitation ice from simulated atmospheric precipitation, impact ice from in-cloud icing and bulk water ice. These are denoted as ice type 1, 2 and 3, respectively, as defined in Table I. All ice was generated with demineralized water of resistivity 18 Ω. The air temperature $T_{air}$ was kept constant at −10°C similar to other studies,[17,23,30–32] while the sample surface temperature was recorded during icing for ice type 1 and 2. Other environmental conditions, such as humidity, were kept constant. An overview of both environmental and icing conditions are found in the supplementary material.

All tests were conducted on bare aluminum 6061-T6 bars polished with Walter BLENDEX Drum fine 0724 M4. The bars had length 340 mm, width 31.8 mm and thickness 6.3 mm, and icing occurred over an area of 1100 mm$^2$ independent of the ice type. The accreted ice had a thickness of 7.5 ± 0.8 mm and a mass of 7 ± 2 g, depending on the type of ice. Before icing, the bars were stored in a cold room so the icing would start with a surface temperature of −10°C.

The experimental protocols for Ice 1 and Ice 2 were standardized at AMIL,[30,33] while the protocol for generating Ice 3 was developed for this study. Ice 1 was created from a freezing drizzle and is denoted as precipitation ice. This ice was generated in a cold room with an air temperature of −10.0 ± 0.2°C and a relative humidity of 80% ± 2% as described elsewhere.[33] Six beams were iced simultaneously with water with a median volume drop diameter (MVD) of 324 μm and at an initial temperature of 4°C. As the water hit the beams, however, it had become super-cooled due to the low ambient temperature. Water impact speed was the free fall value of the droplets in the vertical airflow from an overhead nozzle, which was calculated to be 5.6 ms$^{-1}$. The bars were subjected to the precipitation for 33 minutes, and kept in the cold room for 1 hour between the icing and the centrifuge test to allow the ice to thermally stabilize. The surface temperature of the aluminum during icing was measured to be −6.8 ± 0.1°C. A typical sample of Ice 1 is shown in Fig. 1a. Ice 1 is similar to ice studied in several other publications,[17,33,34] and is typically found in nature after instances of super-cooled rain.

Ice 2, impact ice created from in-cloud icing, was generated by spraying supercooled micro-droplets of water in a closed-loop icing wind tunnel at air temperature −10°C with a wind speed of 15 ms$^{-1}$, liquid water content (LWC) of 2.5 gm$^{-3}$ and MVD of 27 ± 3 μm. The choice of these parameters was elaborated elsewhere,[33] as part of the standardized procedures at AMIL. The aluminum bars were placed upright in the wind tunnel, with seven to nine bars in each test. Everything except the icing area was shielded by a screen during icing. The icing time was 8 minutes and 15 seconds for all ice generated in the wind tunnel. The surface temperature of the aluminum during icing was measured to be −9.1 ± 0.3°C. The bars were kept in the cold room for 1 hour of waiting time between the icing and the centrifuge test. The resulting ice can be seen in Fig. 1b. Ice 2 is similar to other ice generated in a wind tunnel.[20,30,35–37] Such ice is typically found after super-cooled rain coupled with high wind speeds, such as on ships and large structures after storms.

Ice 3, or bulk water ice, was assumed similar to clear ice such as found in ice cubes, and was generated by freezing water with a starting temperature of 4°C in silicon molds. The silicon molds
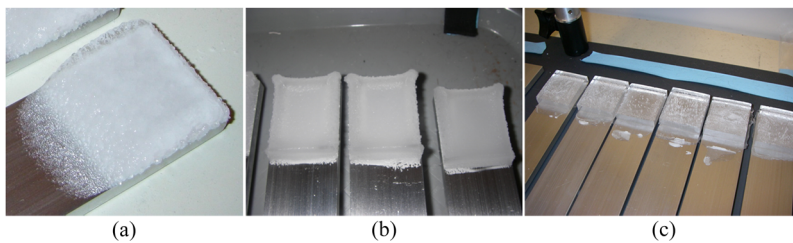


FIG. 1. Images of the different types of ice used in this investigation. (a) Ice 1. (b) Ice 2. (c) Ice 3.

(a)          (b)          (c)

were created from MoldMax30 by Smooth-On,[38] and the conditions in the cold room were the same as for Ice 1. The aluminum bars were placed at the water interface of the silicon molds at the same time as the water insertion, and the bars had an initial temperature of −10°C. To investigate the effect of the initial temperature difference between the inserted water and the aluminum bars, two measurement series were performed, where both the water and the bars had the initial temperature of 4°C at start of freezing. Each silicon mold contained 10 ml of water, and had the same dimensions as the iced area of the bars. The icing time varied from 2 hours to 3 hours and 15 minutes. The bars were spun in the centrifuge immediately after the mold was removed. Due to the inability to distinguish between the samples with different initial water temperatures and icing time, it can be concluded that these parameters do not impact the ice adhesion strength. Six bars were iced simultaneously for each measurement series. Typical samples of Ice 3 is found in Fig. 1c. Ice cubes similar to Ice 3 have been studied in several other investigations.[13,15,18,19,23,31,32,39–41] This type of ice is often found when the temperature has dropped rapidly in an available body of water.

Before the centrifuge test, the mass and thickness of the accreted ice were measured. Each sample was spun individually in the centrifuge. The mass and dimensions of each aluminum bar were known, which made it possible to find the exact mass and thickness of the accreted ice. The total mass of the accreted ice and aluminum bar was measured both immediately before and after the centrifuge test, to calculate the mass of the detached ice. The mass was measured in grams on a digital scale. The thickness of the accreted ice was measured with a vernier caliper right before spinning. Because the thickness of the ice samples varies from one end to the other as seen in Fig. 1, especially for Ice 1 in Fig. 1a, all the thickness measurements were conducted on the thickest part of the ice samples. This protocol gives a higher experimental uncertainty for Ice 1 than Ice 2 and Ice 3. The uncertainties of the mass and thickness measurements are further discussed in Section IV A.

As the centrifuge was placed inside the cold room at −10°C, there was no thermal variation associated with the centrifuge test. The specimen was kept in −10°C for at least one hour prior to spinning, which was sufficient for the sample temperature to stabilize. Consequently, it is reasonable to assume that there was no difference in the temperature of the ice-solid interface between the different samples. Moreover, the temperature of a control sample was monitored with a thermocouple during the waiting time before spinning to ensure that all latent heat from the solidification of water had left the ice samples.

All measurements of the mass and thickness of the ice samples were taken right before the centrifuge adhesion test. The short amount of time between the measurements of the ice samples and the ice adhesion test lessens the effect of sublimation, which might otherwise have resulted in a substantial error in the measurements of the ice samples compared to the measured ice adhesion strength.

## B. Centrifugal adhesion test

The ice adhesion strength is measured with centrifugal force in a CAT apparatus, which consists of a centrifuge, the placed sample beam, and a cover as seen in Fig. 2.[33] A counterweight was applied



**FIG. 2**. The centrifuge adhesion test set-up with the centrifuge at position a, the iced beam at position b and the cover with the piezoelectric cells at position c.

to the opposite end to balance the beam during spinning. The balanced and iced bars were spun in the centrifuge at an accelerating speed of 300 rpms$^{-1}$ between 0 and 30 seconds until the ice was detached by the centrifugal force. At this strain rate, calculated to be about $\dot{\varepsilon} = 10^{-6}$, polycrystalline ice displays brittle behavior.[33] Piezoelectric cells situated around the centrifuge cover instantly detected the detachment of the ice. The rotation speed at the time of the ice detachment was recorded. The ice adhesion strength corresponds to the centrifugal shear stress at the position of the ice sample at the moment of detachment. The ice adhesion strength $\tau$ is thus given by

$$\tau = \frac{F}{A} = \frac{m_{ice}\omega^2 r}{A}, \quad (1)$$

where $F$ is the centrifugal force, $m_{ice}$ is the mass of the detached ice, $\omega$ is the angular velocity at the time of detachment, $r$ is the radius of the beam at the center of mass for the accreted ice and $A$ is the surface area of the detached ice.

The test was discarded if a cohesive break occurs. Such a cohesive break is not frequent with the CAT apparatus, but can occur under certain circumstances.[33] All the samples included in this study showed full adhesive failure, with no ice left on the bars after removal.

The accuracy of the CAT apparatus in terms of correctly determining the ice adhesion strength is among the most accurate in the field.[42] The piezoelectric cells ensure determination of the exact detachment speed, which uniquely calculates the ice adhesion strength. The error from the piezoelectric cells is negligible, and is not separated out in the final error analysis but rather incorporated in the standard deviation of the measurements.
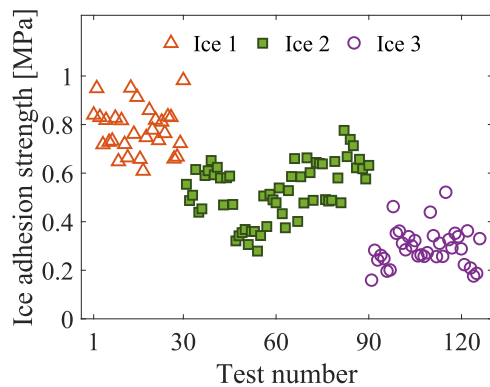
FIG. 3. Ice adhesion strength for the three ice types.

## III. RESULTS

A total of 126 measurements are included in this analysis. See supplementary material for more information on the individual tests. The number of measurements per ice type were 30 for Ice 1, 60 for Ice 2 and 36 for ice type 3.

The ice adhesion strength is displayed in Fig. 3 for all tests. This figure shows a significant difference in ice adhesion strength for the three ice types. It can also be seen that the ice adhesion strength varies considerably within all three ice types, with large standard deviations (see supplementary material). Such variations are to be expected, as the ice will crystallize in a random manner for each sample. The variation is larger for Ice 2, which was generated in a wind tunnel, indicating that this ice generation method has a larger inherent variance than other types of ice.

The mean ice adhesion strength for the three ice types is shown in Table II together with the standard deviation. Table II also shows the ice adhesion strength relative to Ice 1, and it can be seen that the ice adhesion strength for Ice 3 is less than 40% of that for Ice 1. Although the standard deviation is up to 30%, the trend of decrease in ice adhesion strength from Ice 1 to Ice 3 is clear.

## IV. DISCUSSION

### A. Effect of experimental parameters and ice density

The only relevant parameters differentiating ice adhesion strengths between ice types is the ice formation process, i.e. the corresponding ice types and their micro-structure.

**TABLE II**. Mean ice adhesion strength for the three types of ice, including the standard deviation. The percentage of ice adhesion strength relative to Ice 1 are also shown, with $\tau$ and $\tau_{Ice\,1}$ as the ice adhesion strength of the ice type and Ice 1.

| Ice type | Mean ice adhesion strength [MPa] | Standard deviation [MPa (%)] | $\tau/\tau_{Ice\,1}$ |
|---|---|---|---|
| Ice 1 | 0.780 | ±0.102 (13.1%) | 100% |
| Ice 2 | 0.529 | ±0.119 (22.5%) | 68% |
| Ice 3 | 0.284 | ±0.083 (28.2%) | 36% |

Under different icing conditions, the micro-structure and density of the accreted ice change. The importance of changing density for accreted ice and ice properties has been investigated in several publications.[28,43–51] In this study, the density of the ice is approximated by the ratio of the mass to the thickness of the ice, as the area of the aluminum bars exposed to icing is the same for all ice types resulting in an approximately equal icing area. This approximation of the density is denoted as apparent density.

Uncertainties in the apparent density are a combination of the uncertainty in the mass of the detached ice and the maximum thickness of the ice samples. However, neither the uncertainty from the digital weight, the uncertainty from the vernier caliper, nor the uncertainty from the varying thickness of the ice samples are included in the error analysis of the apparent density. As the use of the apparent density is an approximated parameter to discuss the actual density of the ice, the added uncertainty of the apparent density calculations has been omitted for simplicity. When these observations are repeated or expanded in a later study, these uncertainties must be accounted for in a systematic fashion to ensure that the discussion includes the actual density of the different ice types.

In Fig. 4, the mean ice adhesion strength for each ice type is shown as a function of the mass divided by the thickness. In this figure, the three ice types are clearly differentiated by their apparent density. This observation is in accordance with other studies.[28,44–46,48,51] It can be seen from Fig. 4 that a higher apparent density indicates a lower ice adhesion strength.

Although the results from the large number of tests indicate a relation between density and ice adhesion strength, the number of tests are not sufficiently large to result in a predictive model. When a best fit function is forced, it becomes overfitted and thus non-predictive. However, there is a significant relationship between the apparent density and the ice adhesion strength as shown by P-values in supplementary material. To indicate the relation, a best-fit linear model for the adhesion strength as function of density based on all performed experiments became

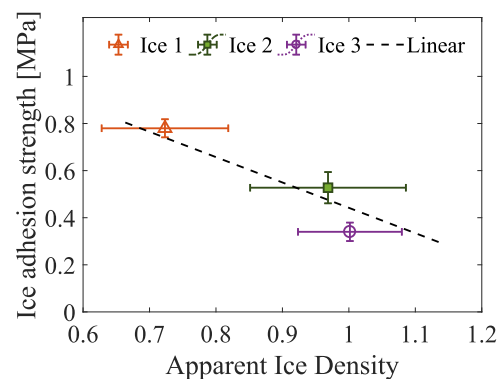$$\tau = -0.0015 \times 10^{-3} \rho' + 1.7811, \qquad (2)$$



FIG. 4. Mean ice adhesion strength per ice type as a function of mass per ice thickness, i.e. apparent density, with standard deviations included. The linear fitting is given by equation (2), and is calculated from all experimental data (see supplementary material).

where $\tau$ is the ice adhesion strength in MPa, and $\rho'$ is the ice density in kgm$^{-3}$. The ice density $\rho'$ is calculated as the ratio of apparent density in gmm$^{-1}$ to the icing area $A = 1100$ mm$^2$, which is constant for all ice types. The linear relation for ice adhesion strength in equation (2) is given as a function of the ice density $\rho'$ instead of apparent density to make the relation applicable for testing by other research groups in SI-units.

The significance of the linear relation decreases when subsets of the experimental data points are considered compared to the linear relation in equation (2) where all observations are included (see supplementary material). Both quadratic and exponential models show similar or less correlation than linear models, but as the exact relation is unknown at this time the simplest linear relation is shown. Further research is needed to establish the exact correlation between ice adhesion strength and density of different ice types and more variables, such as icing conditions. It is important to remember that such an improved relation might not be linear.

The results in this study are preliminary, and only deal with apparent density as compared to actual density. The authors plan to conduct further studies, which will increase the insight into the relation between the ice density and ice adhesion strength for all three types of accreted ice.

### B. Properties of the ice

The three ice types included in this study are all composed of ice Ih, as they are all obtained by freezing water at atmospheric pressure in a temperature above $-100°$C.[4] Ice Ih crystallizes in a hexagonal lattice, where the molecules are linked to each other with hydrogen bonds.

The porosity of sea ice is a function of density, temperature and salinity.[52] For zero salinity, as in de-mineralized water, and at constant temperature, the porosity of ice will depend on density alone. For the rest of this paper, the term porosity will therefore be inversely equivalent to the ice density.

The density of the three types of ice are all dependent on the fraction of air volume. From Fig. 4, it is seen that Ice 1 has the lowest density, followed by Ice 2 and then Ice 3. The opacity of the ice is also a measure of the density of the ice, as a higher fraction of air bubbles in the ice results in a more opaque ice.[53] From Fig. 1a, it is clear that Ice 1 has a much higher degree of air bubbles present than the other types of ice, and that Ice 3 in Fig. 1c is almost completely free of air bubbles. The different transparencies of the ices substantiates the different densities of the ice types as seen in Fig. 4.

The ice type with the highest theoretical density is often denoted as glaze ice, due to the lack of air bubbles in the ice[25,45] compared to other ice types such as for instance freezing drizzle, hail, hoarfrost, rime, and others.[54] The exact definition of glaze ice varies,[25,42,54] but it can be assumed that Ice 3 displays a structure similar to that of theoretical glaze ice due to the high transparency and the lack of air bubbles.[53] Micro-structures of the ice types might be proposed based on the densities, and such proposed structures can be found in the supplementary material.

The density of accreted ice depends on both temperature and the droplet impact velocity, and has been found to increase with the increase of impact velocity and droplet size.[28] For low impact velocity the droplets retain their spherical shapes and form an open ice structure of low densities when freezing. At $-10°$C, droplets

start merging together, but are still individually discernible.[28] For higher impact velocity, the droplets start fusing together, mostly by a spreading in liquid state over the underlying ice. Such a process increases the density of the ice. At similar temperatures, the only difference in density will be due to the impact velocity. With respect to the processes described, the micro-structure of Ice 1 and Ice 2 should be similar to the proposed micro-structures.

It is worth mentioning that when the iced surface area is assumed constant and equal to the surface area of the detached ice, the density of the ice types fits well with the predictions of previous studies on density of ice types,[28] although slightly elevated compared to what is expected (see supplementary material).

### C. Comparison with analytical models

The ice adhesion results obtained in this investigation match previous experiments.[22,55] Several analytical models have tried to explain the mechanisms of ice adhesion. One model explains ice adhesion through electrostatic interactions,[25] while another explains ice adhesion through the existence of a liquid-like layer at the ice-solid interface.[34] These models are further described in supplementary material.

Both analytical models include different ice types in their equations, but when the parameters from this study are tested, the models give predictions that are in direct contrast with the experimental results. The electrostatic model gives a lower ice adhesion strength for lower densities,[25] which would mean that Ice 1 should have a lower ice adhesion strength than Ice 3. For the model based on the liquid-like layer in the ice-solid interface,[34] the calculations predict that the ice adhesion strength of Ice 2 should be higher than the ice adhesion strength of Ice 1. It is clear from Fig. 3 that neither trend is observed. It can be concluded that the existing models do not take different ice types sufficiently into account. To increase the predictability of models, new models of ice adhesion strength should be tested with several different types of ice to be as general as possible.

### D. Possible mechanisms

So far, there is no clear explanation as to why the different ice types behave as observed in the experiments performed in this study. In addition, the mechanisms governing the ice detachment during ice adhesion tests are strongly coupled. The mechanical properties of ice are directly related to their micro-structure. In this section, some of the factors which might influence the ice detachment of the three different ices are described and briefly discussed. These factors should be included in further studies to predict the ice adhesion strength of different ice types and explain their detachment mechanisms.

The micro-structure of ice is determined during the crystallization process. Icing can generally be divided into wet icing and dry icing,[5,56] which are separated by the amount of available water during freezing. For dry icing, such as Ice 1 and Ice 2, the density is lower than for wet icing,[5] such as Ice 3. In addition, the crystallization process is influenced by the heat balance of the icing,[57] which varies for different icing conditions.

The stiffness and elastic modulus of ice and the ice porosity have a negative linear relationship for a given grain size,[58,59] such that a higher density results in a higher cohesive stiffness of the ice.

It has been suggested that hydrogen bonds greatly influence the ice adhesion strength,[40] which is consistent with the stiffening of the ice at higher densities due to a shortening hydrogen bond.[60,61] A consequence of this stiffening is that Ice 3 is stiffer than the other ice types, due to a higher density. The higher stiffness might be a factor for the lower ice adhesion strength observed, similar to that found in the adhesion of geckos.[62]

There are two relevant length scales in freshwater ice which affects the fracture behavior, namely the grain size and the ice thickness.[63,64] As such, the most important factor for the detachment behavior is likely the grain size distribution. An increase of grain size reduces the strength of the ice.[5] There are larger stress concentrations in front of larger crystal grains, and grain sizes influence whether the failure of ice is brittle or ductile at a given strain rate $\dot{\varepsilon}$.[65–67] Furthermore, the density of micro-cracks is proportional to the grain size,[68] giving more faults in ices with larger grain sizes.

Another important factor which influences the ice adhesion strength is the temperature at the ice and surface interface. However, in this study, this factor can be excluded due to the same air temperature for all tests and the inability to distinguish the instances of Ice 3 where a different initial water temperature was utilized.

Further research is required to explore the difference in ice detachment mechanisms for the three ice types. As several of the potential influencing factors depend on the grain sizes, it is important to understand the role of grain size on the ice adhesion. The relevant detachment processes could also be investigated computationally, similarly to previous simulations of ice adhesion.[69–71] Such knowledge could lead to the improvement of anti-icing surfaces by specializing the detachment process of ice.

## V. CONCLUDING REMARKS

Ice and frost cause inconvenience for daily life, and can have potentially catastrophic consequences. One of the promising anti-icing strategies is the reduction of ice adhesion. Unlike previous studies focusing on the development of icephobic surfaces, this investigation is an attempt on the impact of different types of ice on the ice adhesion properties for the same substrate and environmental conditions. The ice types included in the investigation were precipitation ice created in a cold room with water droplets raining, in-cloud ice generated in a wind tunnel, and bulk water ice frozen directly onto the bars with silicon molds. The ice was frozen on identical aluminum 6061-T6 bars, and ice adhesion strength was measured with the centrifuge adhesion test. A relation was found between the mass per thickness of the generated ice and the ice adhesion strength. From this relation, it is seen that the ice adhesion strength decreases for an increasing density of the generated ice. Ice 3, which was the ice type with the highest density, was found to have an ice adhesion strength of less than 40% of that of Ice 1, which was hardest to remove. It appears that ice stiffness or porosity plays an unexpected role in ice adhesion strength and more studies are definitely needed to depict the effect of icing process on the resulting adhesion mechanisms. If correct, these observations may inspire a new strategy in icephobic surfaces, specifically tailored to the ice which is desired removed.

## SUPPLEMENTARY MATERIAL

Supplementary material available, including full experimental results, information about statistical analysis, proposed microstructures for the ice types, and comparison of results with analytical models.

## ACKNOWLEDGMENTS

## REFERENCES

[1] J. Lv, Y. Song, L. Jiang, and J. Wang, "Bio-inspired strategies for anti-icing," ACS Nano **8**, 3152–3169 (2014).

[2] K. Mittal, "Editorial note," Journal of Adhesion Science and Technology **26**, 405–406 (2012).

[3] D. K. Sarkar, "Guest editorial," Journal of Adhesion Science and Technology **26**, 407–411 (2012).

[4] V. F. Petrenko and R. W. Whitworth, *Physics of ice* (Oxford University Press, Great Britain, 2006).

[5] S. Løset, K. N. Shkhinek, O. T. Gudmestad, and K. V. Høyland, *Actions from Ice on Arctic Offshore and Coastal Structures: Student's Book for Institutes of Higher Education* (LAN, St. Petersburg, 2006), p. 277.

[6] V. F. Petrenko, "The effect of static electric fields on ice friction," Journal of Applied Physics **76** (1994).

[7] L. Makkonen, "Modeling power line icing in freezing precipitation," Atmospheric Research **46**, 131–142 (1998).

[8] L. Makkonen, T. Laakso, M. Marjaniemi, and K. J. Finstad, "Modelling and prevention of ice accretion on wind turbines," Wind Engineering **25**, 3–21 (2001).

[9] M. J. Kreder, J. Alvarenga, P. Kim, and J. Aizenberg, "Design of anti-icing surfaces: Smooth, textured or slippery?," Nature Reviews Materials **1**, 1–15 (2016).

[10] L. Makkonen, "Ice adhesion—Theory, measurements and countermeasures," Journal of Adhesion Science and Technology **26**, 413–445 (2012).

[11] R. W. Gent, N. P. Dart, and J. T. Cansdale, "Aircraft icing," Phil. Trans. R. Soc. Lond. A **358**, 2873–2911 (2000).

[12] F. T. Lynch and A. Khodadoust, "Effects of ice accretions on aircraft aerodynamics," Progress in Aerospace Sciences **37**, 669–767 (2001).

[13] V. Hejazi, K. Sobolev, and M. Nosonovsky, "From superhydrophobicity to icephobicity: Forces and interaction analysis," Scientific Reports **3**, 2194 (2013).

[14] H. Sojoudi, M. Wang, N. D. Boscher, G. H. McKinley, and K. K. Gleason, "Durable and scalable icephobic surfaces: Similarities and distinctions from superhydrophobic surfaces," Soft Matter **12**, 1938–1963 (2016).

[15] Z. He, S. Xiao, H. Gao, J. He, and Z. Zhang, "Multiscale crack initiators promoted super-low ice adhesion surfaces," Soft Matter (2017).

[16] K. K. Varanasi, T. Deng, J. D. Smith, M. Hsu, and N. Bhate, "Frost formation and ice adhesion on superhydrophobic surfaces," Appl. Phys. Lett. **97**, 234102–234103 (2010).

[17] A. Dotan, H. Dodiuk, C. Laforte, and S. Kenig, "The relationship between water wetting and ice adhesion," Journal of Adhesion Science and Technology **23**, 1907–1915 (2009).

[18] J. Chen, J. Liu, M. He, K. Li, D. Cui, Q. Zhang, X. Zeng, Y. Zhang, J. Wang, and Y. Song, "Superhydrophobic surfaces cannot reduce ice adhesion," Applied Physics Letters **101**, 111603 (2012).

[19] D. L. Beemer, W. Wang, and A. K. Kota, "Durable gels with ultra-low adhesion to ice," Journal of Materials Chemistry A **4**, 18253 (2016).

[20] M. Schulz and M. Sinapius, "Evaluation of different ice adhesion tests for mechanical deicing systems" (2015).

[21] M. R. Kasaai and M. Farzaneh, "A critical review of evaluation methods of ice adhesion," 23rd International Conference on Offshore Mechanics and Arctic Engineering **3**, 919–926 (2004).

[22] D. N. Anderson and A. D. Reich, "Tests of the performance of coatings for low ice adhesion," Technical Memorandum 107399, 14 (1997).

[23] A. J. Meuler, J. D. Smith, K. K. Varanasi, J. M. Mabry, G. H. McKinley, and R. E. Cohen, "Relationships between water wettability and ice adhesion," ACS Applied Materials & Interfaces **2**, 3100–3110 (2010).

[24] C. Wang, W. Zhang, A. Siva, D. Tiea, and K. J. Wynne, "Laboratory test for ice adhesion strength using commercial instrumentation," Langmuir **30**, 540–547 (2014).

[25] G. Fortin and J. Perron, "Ice adhesion models to predict shear stress at shedding," Journal of Adhesion Science and Technology **26**, 523–553 (2012).

[26] M. Javan-Mashmool, C. Volat, and M. Farzaneh, "A new method for measuring ice adhesion strength at an ice–substrate interface," Hydrological Processes **20**, 645–655 (2006).

[27] J. M. Sayward, "Seeking low ice adhesion," Report (U.S. Army Cold Regions Research and Engineering Laboratory, 72 Lyme Road, Hanover, NH, USA, 03755-1290, 1979).

[28] W. C. Macklin, "The density and structure of ice formed by accretion," Quarterly Journal of the Royal Meteorological Society **88**, 30–50 (1962).

[29] A. Icing, Materials International Laboratory (AMIL), Available from http://amillaboratory.ca/about-us/ and http://amillaboratory.ca/about-us/accreditations/ [Accessed January 29 2019].

[30] S. A. Kulinich and M. Farzaneh, "Ice adhesion on super-hydrophobic surfaces," Applied Surface Science **255**, 8153–8157 (2009).

[31] K. Golovin, S. P. R. Kobaku, D. H. Lee, E. T. DiLoreto, J. M. Mabry, and A. Tuteja, "Designing durable icephobic surfaces," Science Advances **2** (2016).

[32] K. Golovin and A. Tuteja, "A predictive framework for the design and fabrication of icephobic polymers," Science Advances **3** (2017).

[33] C. Laforte and A. Beisswenger, "Icephobic material centrifuge adhesion test," in *11th International Workshop on Atmospheric Icing on Structures (IWAIS)* (2005), pp. 1–5.

[34] F. Guerin, C. Laforte, M.-I. Farinas, and J. Perron, "Analytical model based on experimental data of centrifuge ice adhesion tests with different substrates," Cold Regions Science and Technology **121**, 93–99 (2016).

[35] S. A. Kulinich, S. Farhadi, K. Nose, and X. W. Du, "Superhydrophobic surfaces: Are they really ice-repellent?," Langmuir **27**, 25–29 (2011).

[36] S. A. Kulinich and M. Farzaneh, "How wetting hysteresis influences ice adhesion strength on superhydrophobic surfaces," Langmuir **25**, 8854–8856 (2009).

[37] S. A. Kulinich and M. Farzaneh, "On ice-releasing properties of rough hydrophobic coatings," Cold Regions Science and Technology **65**, 60–64 (2011).

[38] Smooth-On, Inc., 5600 Lower Macungie Road, Macungie, PA 18062, USA, "Mold max™ series tin cure silicone mold making rubber," Available from https://www.smooth-on.com/product-line/mold-max/ [Accessed February 08 2018] (2018).

[39] Z. He, E. T. Vågenes, C. Delabahan, J. He, and Z. Zhang, "Room temperature characteristics of polymer-based low ice adhesion surfaces," Scientific Reports **7**, 42181 (2017).

[40] K. Matsumoto, D. Tsubaki, K. Sekine, H. Kubota, K. Minamiya, and S. Yamanaka, "Influences of number of hydroxyl groups and cooling solid surface temperature on ice adhesion force," International Journal of Refrigeration **75**, 322–330 (2017).

[41] L. E. Raraty and D. Tabor, "The adhesion and strength properties of ice," Proceedings the Royal of Society A: Mathematical Physical & Engineering Sciences **245**, 184–201 (1958).

[42] A. Work and Y. Lian, "A critical review of the measurement of ice adhesion to solid substrates," Progress in Aerospace Sciences **98**, 1–26 (2018).

[43] G. W. Timco and R. M. W. Frederking, "A review of sea ice density," Cold Regions Science and Technology **24**, 1–6 (1996).

[44] K. F. Jones, "The density of natural ice accretions related to nondimensional icing parameters," Quarterly Journal of the Royal Meteorological Society **116**, 477–496 (1990).

[45] G.-L. Lei, W. Dong, M. Zheng, Z.-Q. Guo, and Y.-Z. Liu, "Numerical investigation on heat transfer and melting process of ice with different porosities," International Journal of Heat and Mass Transfer **107**, 934–944 (2017).

[46] F. Prodi, L. Levi, and P. Pederzoli, "The density of accreted ice," Quarterly Journal of the Royal Meteorological Society **112**, 1081–1090 (1986).

[47] M. Rios, "Icing simulations using Jones' density formula for accreted ice and LEWICE," in *29th Aerospace Sciences Meeting*, Aerospace Sciences Meetings (American Institute of Aeronautics and Astronautics, 1991).

[48] P. L. I. Skelton and G. Poots, "The effect of density variations during rime growth on overhead transmission line conductors," Cold Regions Science and Technology **22**, 311–317 (1994).

[49] K. Szilder, "The density and structure of ice accretion predicted by a random-walk model," Quarterly Journal of the Royal Meteorological Society **119**, 907–924 (1993).

[50] K. Szilder and E. P. Lozowski, "Three-dimensional modelling of ice accretion density," Quarterly Journal of the Royal Meteorological Society **126**, 2395–2404 (2000).

[51] M. Vargas, H. Broughton, J. J. Sims, B. Bleeze, and V. Gaines, "Local and total density measurements in ice shapes," Journal of Aircraft **44**, 780–789 (2007).

[52] G. F. N. Cox and W. F. Weeks, "Changes in the salinity and porosity of sea-ice samples during shipping and storage," Journal of Glaciology **32**, 371–375 (1986).

[53] A. E. Carte, "Air bubbles in ice," Proceedings of the Physical Society **77**, 757 (1961).

[54] T. Armstrong, B. Roberts, and C. Swithinbank, *Illustrated Glossary of Snow and Ice* (Scott Polar Research Institute, Cambridge, 1973).

[55] A. Reich, "Interface influences upon ice adhesion to airfoil materials," in *32nd Aerospace Sciences Meeting and Exhibit*, Aerospace Sciences Meetings (American Institute of Aeronautics and Astronautics, 1994).

[56] G. S. H. Lock, *The Growth and Decay of Ice*, Studies in Polar Research (Cambridge University Press, Great Britain, 1990).

[57] L. Yanan, G. Xiaosong, and H. Yecong, "Experimental study on criteria correlation of heat convection between air and wires in icing conditions," in *2013 Fourth International Conference on Digital Manufacturing and Automation*, pp. 591–594.

[58] B. Michel, *Ice Mechanics* (Les Presses De L'Université Laval, Canada, 1978).

[59] D. M. Cole, "Modeling the cyclic loading response of sea ice," International Journal of Solids and Structures **35**, 4067–4075 (1998).

[60] C. Q. Sun, X. Zhang, and W. Zheng, "The hidden force opposing ice compression," Chemical Science **3**, 1455–1460 (2012).

[61] C. Q. Sun, X. Zhang, X. Fu, W. Zheng, J.-l. Kuo, Y. Zhou, Z. Shen, and J. Zhou, "Density and phonon-stiffness anomalies of water and ice in the full temperature range," The Journal of Physical Chemistry Letters **4**, 3238–3244 (2013).

[62] B. I. N. Chen and H. Gao, "An alternative explanation of the effect of humidity in gecko adhesion: Stiffness reduction enhances adhesion on a rough surface," International Journal of Applied Mechanics **02**, 1–9 (2010).

[63] J. P. Dempsey, S. J. Defranco, R. M. Adamson, and S. V. Mulmule, "Scale effects on the in-situ tensile strength and fracture of ice. Part I: Large grained freshwater ice at spray lakes reservoir, Alberta," International Journal of Fracture **95**, 325 (1999).

[64] C. Bu, C. A. Dukes, and R. A. Baragiola, "Spontaneous cracking of amorphous solid water films and the dependence on microporous structure," Applied Physics Letters **109**, 201902 (2016).

[65] R. W. Lee and E. M. Schulson, "The strength and ductility of ice under tension," Journal of Offshore Mechanics and Arctic Engineering **110**, 187–191 (1988).

[66] E. M. Schulson, "The structure and mechanical behavior of ice," JOM **51**, 21–27 (1999).

[67] E. M. Schulson, P. N. Lim, and R. W. Lee, "A brittle to ductile transition in ice under tension," Philosophical Magazine A **49**, 353–363 (1984).

[68] D. M. Cole, "Effect of grain size on the internal fracturing of polycrystalline ice," Report (Cold Region Research and Engineering Lab, Hanover, NH, 1986).

[69] S. Xiao, J. He, and Z. Zhang, "Nanoscale deicing by molecular dynamics simulation," Nanoscale **8**, 14625 (2016).

[70] T. Hynninen, V. Heinonen, C. L. Dias, M. Karttunen, A. S. Foster, and T. Ala-Nissila, "Cutting ice: Nanowire regelation," Physical Review Letters **105** (2010).

[71] C. J. Burnham, J.-C. Li, and M. Leslie, "Molecular dynamics calculations for ice Ih," The Journal of Physical Chemistry B **101**, 6192–6195 (1997).